Radiation Characteristics of Dielectric-Coated Coaxial Waveguide Periodic Slot with Finite and Zero Thickness

Chang-Won Lee and Hyun Son

***Abstract*—The leaky wave radiated from the dielectric coated coaxial waveguide periodic slot with finite and zero thickness is investigated theoretically for the infinite and finite periodic structures. For the infinite periodic structure, mode-matching technique and integral equation method are applied to the analysis of finite and zero thickness slot cases, respectively. The integral equations are derived for the finite periodic structure by use of the Fourier transform and mode expansion and simultaneous linear equations are obtained. The effects of the slot thickness, the finite slot number and the dielectric coating are analyzed. Results for finite periodic slots are compared with those of the infinite extent structure and good agreement is found.**

***Index Terms*—Coaxial waveguide, leaky wave antenna, periodic structure.**

I. Introduction

THE millimeter-wave omnidirectional leaky-wave antenna has been a subject of several investigations because of an increasing need for developing new antenna types to suit the various demands imposed by the millimeter-wave systems. A circular dielectric waveguide with periodic corrugations [1] and a metallic grating loaded circular dielectric waveguide [2] were investigated theoretically and experimentally to produce an omnidirectional leaky-wave antenna when it was excited by the TE_{01} mode in a circular metallic waveguide including $H_{10} - H_{01}$ mode transducer. The leakage constant of the former structure was so small that a long antenna length was required to obtain reasonable antenna efficiency. Thus, the latter structure was investigated to reduce the length of the antenna structure in which a large leakage constant was obtained when it was compared with the previous one [1]. Both structures must have the transducer between excitation circular metallic waveguide and feeder section of the antenna to obtain a circularly symmetrical incident field feeding into the radiator. In this paper, a new omnidirectional leaky-wave antenna is proposed and analyzed to obtain a simpler feeding structure and improve the performance of leaky-wave antennas. This is a dielectric coated coaxial waveguide periodic slot with finite and zero thickness.

The mode-matching technique is applied to the analysis of an infinite periodic slot with a finite thickness and the integral equation method is applied to the infinite extent structure with zero thickness slots. In the mode-matching formulation, the radial waveguide modes are employed to express the fields in the finite thick slot region and space harmonics in other regions. Boundary conditions are imposed at the interfaces and a homogeneous linear equation is obtained. For the zero thickness slot case, the unknown electric current on the metal strip is expanded into a product of a series of cosine functions and a function satisfying edge condition. The same field expansion with the finite thickness slot case is used in each region. From the boundary conditions, a homogeneous linear equation is also obtained. The phase and leakage constants which determine the radiation characteristics of a leaky-wave antenna are calculated by the nontrivial condition of the homogeneous linear equation.

Up to now most studies have been devoted to the characteristic of the infinite periodic geometry and so the feeding and finite effect of the structure have not been taken into account. Hence, a resolution method for the finite slot number case is needed. For this case, fields in slot regions are expressed as a summation of the radial waveguide TM modes, which is similar to the infinite structure and in other regions are expressed in the spectral domain by using the inverse Fourier transformation. Boundary conditions at the interfaces are enforced and the simultaneous linear equations are derived.

The influences of the slot width, slot thickness, and dielectric coating on the radiation characteristics (leakage constant, phase constant, and radiation pattern) are investigated. The effects of the finite slot number and the dielectric coating over the slots are also studied by increasing the total slot number and the dielectric thickness, respectively. The results of the finite periodic slots are compared with those of the infinite extent structure and good agreement has been found. The method presented in this paper can be applied to the analysis of the finite thick metal-grating-loaded circular dielectric leaky-wave antenna.

II. Mode-Matching Formulation for Finite Thick Slot

For the periodic structure shown in Fig. 1(a) with finite thick slots, the fields in each region are expressed in a different way. In region (I), incident and reflected waves in the ρ direction must be considered, and imposing the boundary condition on the inner conductor surface, the electric and magnetic fields for TM polarization are expressed as a summation of space harmonics by (1) and (2), shown at the bottom of the next page, where

$$k_{zn} = k_{z0} + 2n\pi/p$$
$$k_{\rho n}^{(1)} = \sqrt{\epsilon_{r1} k_0^2 - k_{zn}^2}$$
$$k_{z0} = \beta - j\alpha.$$

Manuscript received August 15, 1997; revised May 26, 1998.

The authors are with the Department of Electronics, Kyungpook National University, Taegu, 702-701 Korea.

Publisher Item Identifier S 0018-926X(99)02208-5.

0018–926X/99$10.00 © 1999 IEEE

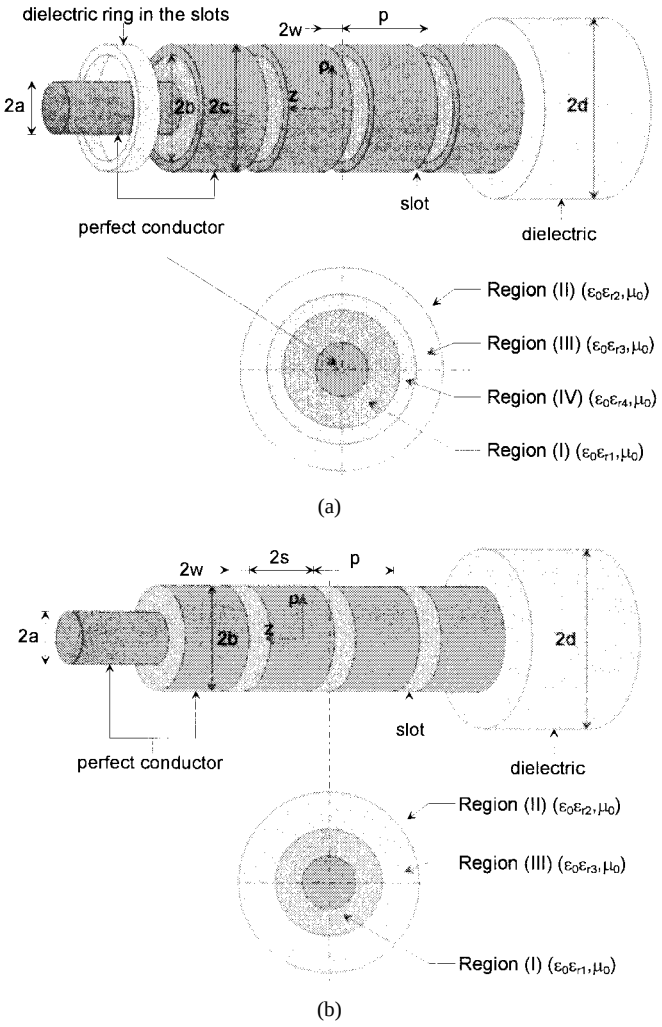

Fig. 1. Geometry of the dielectric covered coaxial waveguide. (a) Structure with finite thickness slot. (b) Structure with zero thickness slot.

$H_n^{(1)}(\cdot)$ is the n order Hankel function of the first kind, A_n are the unknown complex amplitudes of the space harmonics, and k_{zn} is complex propagation constant which must be determined. In region (II), the fields are expressed as a summation of space harmonics and outgoing waves in the ρ direction by

$$H_\phi^{(\mathrm{II})}(\rho, z) = \sum_{n=-\infty}^{\infty} C_n H_1^{(2)}(k_{\rho m}^{(2)}\rho) e^{-jk_{zn}z} \tag{3}$$

$$E_z^{(\mathrm{II})}(\rho, z) = \frac{1}{j\omega\epsilon_0\epsilon_{r2}} \sum_{n=-\infty}^{\infty} C_n k_{\rho m}^{(2)} H_0^{(2)}(k_{\rho m}^{(2)}\rho) e^{-jk_{zn}z} \tag{4}$$

where

$$k_{\rho m}^{(2)} = \sqrt{\epsilon_{r2}k_0^2 - k_{zn}^2}.$$

In region (III), the fields are expressed a summation of space harmonics and standing waves in the ρ direction by

$$H_\phi^{(\mathrm{III})}(\rho, z) = \sum_{n=-\infty}^{\infty} [D_n H_1^{(1)}(k_{\rho m}^{(3)}\rho) + D'_n H_1^{(2)}(k_{\rho m}^{(3)}\rho)] e^{-jk_{zn}z} \tag{5}$$

$$E_z^{(\mathrm{III})}(\rho, z) = \frac{1}{j\omega\epsilon_0\epsilon_{r3}} \sum_{n=-\infty}^{\infty} k_{\rho m}^{(3)} \cdot [D_n H_0^{(1)}(k_{\rho m}^{(3)}\rho) + D'_n H_0^{(2)}(k_{\rho m}^{(3)}\rho)] e^{-jk_{zn}z} \tag{6}$$

where

$$k_{\rho m}^{(3)} = \sqrt{\epsilon_{r3}k_0^2 - k_{zn}^2}.$$

In region (IV), the fields are expressed as a superposition of radial waveguide modes

$$H_\phi^{(\mathrm{IV})}(\rho, z) = \sum_{m=0}^{\infty} \left[B_m \frac{H_1^{(1)}(k_{\rho m}^{(4)}\rho)}{H_1^{(1)}(k_{\rho m}^{(4)}c)} + B'_m \frac{H_1^{(2)}(k_{\rho m}^{(4)}\rho)}{H_1^{(2)}(k_{\rho m}^{(4)}b)} \right] \cdot \cos\frac{m\pi}{2w}(z+w) \tag{7}$$

$$E_z^{(\mathrm{IV})}(\rho, z) = \frac{1}{j\omega\epsilon_0\epsilon_{r4}} \sum_{m=0}^{\infty} k_{\rho m}^{(4)} \cdot \left[B_m \frac{H_0^{(1)}(k_{\rho m}^{(4)}\rho)}{H_1^{(1)}(k_{\rho m}^{(4)}c)} + B'_m \frac{H_0^{(2)}(k_{\rho m}^{(4)}\rho)}{H_1^{(2)}(k_{\rho m}^{(4)}b)} \right] \cdot \cos\frac{m\pi}{2w}(z+w) \tag{8}$$

where

$$k_{\rho m}^{(4)} = \sqrt{\epsilon_{r4}k_0^2 - (m\pi/2w)^2}.$$

B_m and B'_m are the unknown complex amplitudes of radial waveguide modes.

The continuity condition of the tangential electric and magnetic fields is imposed at the interfaces $\rho = b$, $\rho = c$ for $|z| \le w$ and $\rho = d$ for $|z| < p/2$ and the tangential electric field is enforced to be zero on the conductor surfaces. The resulting equations for the electric field are multiplied by the space harmonic functions and integrated over the period. The equations for the magnetic field are multiplied

$$H_\phi^{(\mathrm{I})}(\rho, z) = \sum_{n=-\infty}^{\infty} \frac{A_n}{H_0^{(2)}(k_{\rho m}^{(1)}a)} [H_0^{(2)}(k_{\rho m}^{(1)}a) H_1^{(1)}(k_{\rho m}^{(1)}\rho) - H_0^{(1)}(k_{\rho m}^{(1)}a) H_1^{(2)}(k_{\rho m}^{(1)}\rho)] e^{-jk_{zn}z}, \tag{1}$$

$$E_z^{(\mathrm{I})}(\rho, z) = \frac{1}{j\omega\epsilon_0\epsilon_{r1}} \sum_{n=-\infty}^{\infty} \frac{A_n k_{\rho m}^{(1)}}{H_0^{(2)}(k_{\rho m}^{(1)}a)} [H_0^{(2)}(k_{\rho m}^{(1)}a) H_0^{(1)}(k_{\rho m}^{(1)}\rho) - H_0^{(1)}(k_{\rho m}^{(1)}a) H_0^{(2)}(k_{\rho m}^{(1)}\rho)] e^{-jk_{zn}z} \tag{2}$$

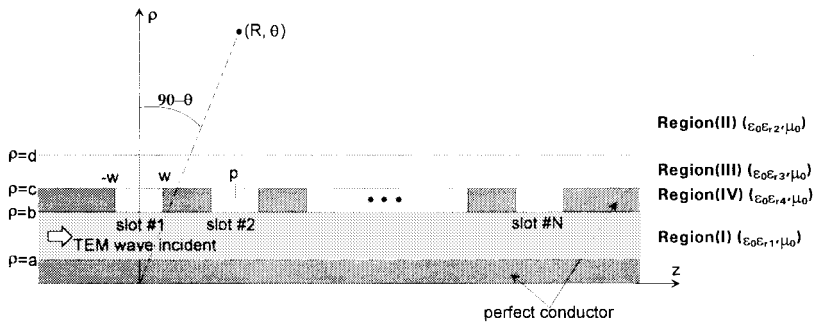

Fig. 2. Geometry of the finite periodic slots.

by radial waveguide modes and integrated over the slot. After considering the orthogonality properties of modes and space harmonics, the following matrix equations are obtained:

$$\mathbf{HB}+\mathbf{B}'=\mathbf{QA} \tag{9}$$

$$\mathbf{PB}+\mathbf{P}'\mathbf{B}'=\mathbf{A} \tag{10}$$

$$\mathbf{B}+\mathbf{G}'\mathbf{B}'=\mathbf{SD}' \tag{11}$$

$$\mathbf{RB}+\mathbf{R}'\mathbf{B}'=\mathbf{D}' \tag{12}$$

where $\mathbf{A}$, $\mathbf{D}'$, $\mathbf{B}$, and $\mathbf{B}'$ are column matrices with the complex amplitudes of space harmonics and radial waveguide modes. $\mathbf{H}$ and $\mathbf{G}'$ are diagonal matrices. The elements of matrices are shown in (13)–(22), shown at the bottom of the page, where δ_{m0} is the Kronecker delta. The relations between $\mathbf{C}$, $\mathbf{D}$, and $\mathbf{D}'$ are given by

$$D_n=R_n^h D_n' \tag{23}$$

$$C_n H_1^{(2)}(k_{\rho n}^{(2)}d)=D_n H_1^{(1)}(k_{\rho n}^{(3)}d)+D_n' H_1^{(2)}(k_{\rho n}^{(3)}d). \tag{24}$$

After some algebraic manipulation, from (9)–(12) the following homogeneous matrix equation is obtained:

$$[\mathbf{I}-\mathbf{SR}-(\mathbf{G}'-\mathbf{SR}')(\mathbf{I}-\mathbf{QP}')^{-1}(\mathbf{H}-\mathbf{QP})]\,\mathbf{B}=0 \tag{25}$$

where $\mathbf{I}$ is the identity matrix. For a nontrivial solution, the determinant of (25) must be zero. From this condition, the unknown complex propagation constant ($\beta-j\alpha$) is calculated. Once $\beta-j\alpha$ is known, the column matrices $\mathbf{B}$, $\mathbf{B}'$, $\mathbf{C}$, $\mathbf{D}$, $\mathbf{D}'$, and $\mathbf{A}$ are obtained by normalization of fundamental mode

---

$$\mathbf{Q}_{mn}=\frac{H_0^{(2)}(k_{\rho n}^{(1)}a)H_1^{(1)}(k_{\rho n}^{(1)}b)-H_0^{(1)}(k_{\rho n}^{(1)}a)H_1^{(2)}(k_{\rho n}^{(1)}b)}{H_0^{(2)}(k_{\rho n}^{(1)}a)}\frac{\nu_{mn}}{(1+\delta_{m0})w} \tag{13}$$

$$\mathbf{H}_{mm}=\frac{H_1^{(1)}(k_{\rho m}^{(4)}b)}{H_1^{(1)}(k_{\rho m}^{(4)}c)} \tag{14}$$

$$\mathbf{P}_{nm}=\frac{\epsilon_{r1}k_{\rho_m}^{(4)}}{p\epsilon_{r4}k_{\rho n}^{(1)}}\frac{H_0^{(2)}(k_{\rho n}^{(1)}a)}{H_0^{(2)}(k_{\rho n}^{(1)}a)H_0^{(1)}(k_{\rho n}^{(1)}b)-H_0^{(1)}(k_{\rho n}^{(1)}a)H_0^{(2)}(k_{\rho n}^{(1)}b)}\frac{H_0^{(1)}(k_{\rho m}^{(4)}b)}{H_1^{(1)}(k_{\rho m}^{(4)}c)}\nu_{mn}^* \tag{15}$$

$$\mathbf{P}'_{nm}=\frac{\epsilon_{r1}k_{\rho_m}^{(4)}}{p\epsilon_{r4}k_{\rho n}^{(1)}}\frac{H_0^{(2)}(k_{\rho n}^{(1)}a)}{H_0^{(2)}(k_{\rho n}^{(1)}a)H_0^{(1)}(k_{\rho n}^{(1)}b)-H_0^{(1)}(k_{\rho n}^{(1)}a)H_0^{(2)}(k_{\rho n}^{(1)}b)}\frac{H_0^{(2)}(k_{\rho m}^{(4)}b)}{H_1^{(2)}(k_{\rho m}^{(4)}b)}\nu_{mn}^* \tag{16}$$

$$\mathbf{S}_{mn}=\left[R_n^h H_1^{(1)}(k_{\rho n}^{(3)}c)+H_1^{(2)}(k_{\rho n}^{(3)}c)\right]\frac{\nu_{mn}}{(1+\delta_{m0})w} \tag{17}$$

$$\mathbf{G}'_{mm}=\frac{H_1^{(2)}(k_{\rho m}^{(4)}c)}{H_1^{(2)}(k_{\rho m}^{(4)}b)} \tag{18}$$

$$\mathbf{R}_{nm}=\frac{\epsilon_{r3}k_{\rho m}^{(4)}}{p\epsilon_{r4}k_{\rho n}^{(3)}}\frac{1}{R_n^h H_0^{(1)}(k_{\rho n}^{(3)}c)+H_0^{(2)}(k_{\rho n}^{(3)}c)}\frac{H_0^{(1)}(k_{\rho m}^{(4)}c)}{H_1^{(1)}(k_{\rho m}^{(4)}c)}\nu_{mn}^* \tag{19}$$

$$\mathbf{R}'_{nm}=\frac{\epsilon_{r3}k_{\rho m}^{(4)}}{p\epsilon_{r4}k_{\rho n}^{(3)}}\frac{1}{R_n^h H_0^{(1)}(k_{\rho n}^{(3)}c)+H_0^{(2)}(k_{\rho n}^{(3)}c)}\frac{H_0^{(2)}(k_{\rho m}^{(4)}c)}{H_1^{(2)}(k_{\rho m}^{(4)}b)}\nu_{mn}^* \tag{20}$$

$$R_n^h=-\frac{\epsilon_{r3}k_{\rho n}^{(2)}H_0^{(2)}(k_{\rho n}^{(2)}d)H_1^{(2)}(k_{\rho n}^{(3)}d)-\epsilon_{r2}k_{\rho n}^{(3)}H_1^{(2)}(k_{\rho n}^{(2)}d)H_0^{(2)}(k_{\rho n}^{(3)}d)}{\epsilon_{r3}k_{\rho n}^{(2)}H_0^{(2)}(k_{\rho n}^{(2)}d)H_1^{(1)}(k_{\rho n}^{(3)}d)-\epsilon_{r2}k_{\rho n}^{(3)}H_1^{(2)}(k_{\rho n}^{(2)}d)H_0^{(1)}(k_{\rho n}^{(3)}d)} \tag{21}$$

$$\nu_{mn}=jk_{zn}\frac{(-1)^m e^{-jk_{zn}w}-e^{jk_{zn}w}}{k_{zn}^2-(m\pi/2w)^2} \tag{22}$$

B_0. The fields in any region are computed by (1)–(8). The far-field radiation pattern is calculated from the known tangential electric fields over each slot by using the equivalence principle. The far-zone magnetic field radiated from a finite section of the infinite structure is given by

$$H_\phi(R,\theta) \approx \frac{-2w\epsilon_{r2}}{\pi\epsilon_{r3}} \sum_{n=-\infty}^{\infty} k_{\rho n}^{(3)}[D_n H_0^{(1)}(k_{\rho n}^{(3)}c) + D_n' H_0^{(2)}(k_{\rho n}^{(3)}c)] \cdot F(k_2\cos\theta)\frac{e^{-jk_2R}}{R}. \tag{26}$$

Here

$$F(\zeta) = \frac{T(\zeta)}{k_{\rho 3}[H_0^{(2)}(k_{\rho 3}c) + R(\zeta)H_0^{(1)}(k_{\rho 3}c)]}\frac{\sin(k_{zn}-\zeta)w}{(k_{zn}-\zeta)w} \cdot \frac{1-e^{j(k_{zn}-\zeta)Mp}}{1-e^{j(k_{zn}-\zeta)p}} \tag{27a}$$

where (27b) is shown at the bottom of the page and M is the total slot number taken into account in a finite section of the infinite periodic structure.

III. Formulation for Zero Thickness Slot

The periodic structure with zero thickness slot is shown in Fig. 1(b), the fields in each region are expressed by (1)–(6). The boundary conditions at $\rho = b$ are given by

$$E_z^{(\mathrm{I})}(b,z) = E_z^{(\mathrm{III})}(b,z) \tag{28}$$

$$H_\phi^{(\mathrm{III})}(b,z) - H_\phi^{(\mathrm{I})}(b,z) = \begin{cases} J_z(z), & |z| \le s \\ 0, & \text{elsewhere} \end{cases} \tag{29}$$

$$E_z^{(\mathrm{III})}(b,z) = 0, \qquad |z| \le s \tag{30}$$

where $J_z(z)$ is the unknown electric current and can be expanded into a product of a series of cosine functions and a function satisfying edge condition [3] as

$$J_z(z) = e^{-jk_{z0}z}\sqrt{1-(z/s)^2}\sum_{\nu=0}^{\infty}(-j)^\nu \mathcal{J}_\nu \cos\omega_\nu(z+s), \qquad \omega_\nu = \nu\pi/2s. \tag{31}$$

The tangential magnetic field boundary condition (29) is multiplied by space-harmonic functions and integrated over the period. The tangential electric field vanishing condition (30) is multiplied by the electric current expansion functions and integrated over strip region. After considering the orthogonality property of space harmonics and some algebraic manipulation, the following homogeneous matrix equation is obtained

$$\mathbf{ZJ} = 0 \tag{32}$$

where

$$\mathbf{Z}_{\mu\nu} = \sum_{n=-\infty}^{\infty}\frac{k_{\rho n}^{(3)}}{\eta_n p}F_{n\nu}F_{n\mu},$$

$$\eta_n = \frac{H_1^{(2)}(k_{\rho n}^{(3)}b) + R_n^h H_1^{(1)}(k_{\rho n}^{(3)}b)}{H_0^{(2)}(k_{\rho n}^{(3)}b) + R_n^h H_0^{(1)}(k_{\rho n}^{(3)}b)} - \frac{\epsilon_{r1}k_{\rho n}^{(3)}}{\epsilon_{r3}k_{\rho n}^{(1)}} \cdot \frac{H_0^{(2)}(k_{\rho n}^{(1)}a)H_1^{(1)}(k_{\rho n}^{(1)}b) - H_0^{(1)}(k_{\rho n}^{(1)}a)H_1^{(2)}(k_{\rho n}^{(1)}b)}{H_0^{(2)}(k_{\rho n}^{(1)}a)H_0^{(1)}(k_{\rho n}^{(1)}b) - H_0^{(1)}(k_{\rho n}^{(1)}a)H_0^{(2)}(k_{\rho n}^{(1)}b)}$$

$$F_{n\nu} = \frac{s\pi}{2}\left[\frac{J_1(2n\pi s/p + \nu\pi/2)}{2n\pi s/p + \nu\pi/2} + (-1)^\nu \cdot \frac{J_1(2n\pi s/p - \nu\pi/2)}{2n\pi s/p - \nu\pi/2}\right]. \tag{33}$$

Here, $J_1(\cdot)$ is the Bessel function of order 1. Similarly, once the unknown complex propagation constant is found by the nontrivial condition of the matrix $\mathbf{Z}$ and then the unknown coefficients of the electric current $\mathcal{J}_\nu$ are obtained. The unknown coefficient of the space-harmonic D_n' are computed by

$$D_n' = \frac{1}{\eta_n[H_0^{(2)}(k_{\rho n}^{(3)}b) + R_n^h H_0^{(1)}(k_{\rho n}^{(3)}b)]p}\sum_{\nu=0}^{\infty}\mathcal{J}_\nu F_{n\nu}$$

and other coefficients are determined by (23) and (24).

IV. Finite N Periodic Slots

A dielectric coated coaxial waveguide with N periodic finite thick slots is shown in Fig. 2. It is assumed that TEM mode is incident in the coaxial waveguide and $(b-a)$ is small enough that only TEM mode is the propagating mode in the coaxial waveguide. The incident fields are

$$E_\rho^i(\rho,z) = \frac{V}{\ln(b/a)\rho}e^{-jk_1z}, \qquad H_\phi^i(\rho,z) = \frac{Vk_1}{\omega\mu_0\ln(b/a)\rho}e^{-jk_1z}. \tag{34}$$

The scattered fields in region (I) which satisfy the boundary condition at $\rho = a$ are expressed (by use of the inverse Fourier

$$R(\zeta) = -\frac{\epsilon_{r2}k_{\rho 3}H_1^{(2)}(k_{\rho 2}d)H_0^{(2)}(k_{\rho 3}d) - \epsilon_{r3}k_{\rho 2}H_0^{(2)}(k_{\rho 2}d)H_1^{(2)}(k_{\rho 3}d)}{\epsilon_{r2}k_{\rho 3}H_1^{(2)}(k_{\rho 2}d)H_0^{(1)}(k_{\rho 3}d) - \epsilon_{r3}k_{\rho 2}H_0^{(2)}(k_{\rho 2}d)H_1^{(1)}(k_{\rho 3}d)}$$

$$T(\zeta) = \frac{\epsilon_{r2}4j/\pi d}{\epsilon_{r2}k_{\rho 3}H_1^{(2)}(k_{\rho 2}d)H_0^{(1)}(k_{\rho 3}d) - \epsilon_{r3}k_{\rho 2}H_0^{(2)}(k_{\rho 2}d)H_1^{(1)}(k_{\rho 3}d)}$$

$$k_{\rho 2} = \sqrt{\epsilon_{r2}k_0^2 - \zeta^2}, \qquad k_{\rho 3} = \sqrt{\epsilon_{r3}k_0^2 - \zeta^2} \tag{27b}$$

transform) as

$$H_\phi^{s(\mathrm{I})}(\rho, z) = \frac{1}{2\pi}\int_{-\infty}^{\infty} \tilde{H}_\phi^{s(\mathrm{I})}(\zeta) \cdot \left[H_1^{(2)}(k_{\rho 1}\rho) - \frac{H_0^{(2)}(k_{\rho 1}a)}{H_0^{(1)}(k_{\rho 1}a)} H_1^{(1)}(k_{\rho 1}\rho)\right] e^{-j\zeta z}\, d\zeta$$

$$E_z^{s(\mathrm{I})}(\rho, z) = \frac{1}{2\pi j\omega\epsilon_0\epsilon_{r1}}\int_{-\infty}^{\infty} \tilde{H}_\phi^{s(\mathrm{I})}(\zeta) k_{\rho 1} \cdot \left[H_0^{(2)}(k_{\rho 1}\rho) - \frac{H_0^{(2)}(k_{\rho 1}a)}{H_0^{(1)}(k_{\rho 1}a)} H_0^{(1)}(k_{\rho 1}\rho)\right] e^{-j\zeta z}\, d\zeta \tag{35}$$

where $k_{\rho 1} = \sqrt{k_1^2 - \zeta^2}$. In region (II), the fields are expressed as a superposition of outgoing waves in the ρ direction

$$H_\phi^{(\mathrm{II})}(\rho, z) = \frac{1}{2\pi}\int_{-\infty}^{\infty} \tilde{H}_\phi^{(\mathrm{III})}(\zeta) T(\zeta) H_1^{(2)}(k_{\rho 2}\rho) e^{-j\zeta z}\, d\zeta$$

$$E_z^{(\mathrm{II})}(\rho, z) = \frac{1}{2\pi j\omega\epsilon_0\epsilon_{r2}}\int_{-\infty}^{\infty} \tilde{H}_\phi^{(\mathrm{III})}(\zeta) T(\zeta) k_{\rho 2} H_0^{(2)}(k_{\rho 2}\rho) \cdot e^{-j\zeta z}\, d\zeta \tag{36}$$

where $k_{\rho 2} = \sqrt{k_2^2 - \zeta^2}$. The fields in region (III) are expressed as a superposition of standing waves in the ρ direction

$$H_\phi^{(\mathrm{III})}(\rho, z) = \frac{1}{2\pi}\int_{-\infty}^{\infty} \tilde{H}_\phi^{(\mathrm{III})}(\zeta) \cdot [H_1^{(2)}(k_{\rho 3}\rho) + R(\zeta) H_1^{(1)}(k_{\rho 3}\rho)] e^{-j\zeta z}\, d\zeta$$

$$E_z^{(\mathrm{III})}(\rho, z) = \frac{1}{2\pi j\omega\epsilon_0\epsilon_{r3}}\int_{-\infty}^{\infty} \tilde{H}_\phi^{(\mathrm{III})}(\zeta) k_{\rho 3} \cdot [H_0^{(2)}(k_{\rho 3}\rho) + R(\zeta) H_0^{(1)}(k_{\rho 3}\rho)] e^{-j\zeta z}\, d\zeta \tag{37}$$

where $k_{\rho 3} = \sqrt{k_3^2 - \zeta^2}$. In region (IV), the fields in the lth slot region are expressed as a summation of radial waveguide TM modes

$$H_\phi^{(\mathrm{IV})}(\rho, z) = \sum_{m=0}^{\infty} \cos w_m(z + w - lp) \cdot \left[b_m^l \frac{H_1^{(1)}(k_{\rho 4m}\rho)}{H_1^{(1)}(k_{\rho 4m}c)} + c_m^l \frac{H_1^{(2)}(k_{\rho 4m}\rho)}{H_1^{(2)}(k_{\rho 4m}b)}\right]$$

$$E_z^{(\mathrm{IV})}(\rho, z) = \frac{1}{j\omega\epsilon_0\epsilon_{r4}}\sum_{m=0}^{\infty} \cos w_m(z + w - lp) k_{\rho 4m} \cdot \left[b_m^l \frac{H_0^{(1)}(k_{\rho 4m}\rho)}{H_1^{(1)}(k_{\rho 4m}c)} + c_m^l \frac{H_0^{(2)}(k_{\rho 4m}\rho)}{H_1^{(2)}(k_{\rho 4m}b)}\right] \tag{38}$$

where $k_{\rho 4m} = \sqrt{k_4^2 - w_m^2}$ and $w_m = m\pi/2w$. The tangential fields continuities at $\rho = d$ are already satisfied by introducing $R(\zeta)$ and $T(\zeta)$. The continuity condition of the tangential electric field through the slots at $\rho = b$ yields

$$\tilde{H}_\phi^{s(\mathrm{I})}(\zeta) = \frac{\epsilon_{r1}}{k_{\rho 1} M_e(\zeta)} \sum_{l=0}^{N-1}\sum_{m=0}^{\infty} \frac{k_{\rho 4m}}{\epsilon_{r4}} Q_l^m(\zeta) \cdot \left[b_m^l \frac{H_0^{(1)}(k_{\rho 4m}b)}{H_1^{(1)}(k_{\rho 4m}c)} + c_m^l \frac{H_0^{(2)}(k_{\rho 4m}b)}{H_1^{(2)}(k_{\rho 4m}b)}\right] \tag{39}$$

where

$$M_e(\zeta) = H_0^{(2)}(k_{\rho 1}b) - \frac{H_0^{(2)}(k_{\rho 1}a)}{H_0^{(1)}(k_{\rho 1}a)} H_0^{(1)}(k_{\rho 1}b)$$

$$Q_l^m(\zeta) = \frac{-j\zeta[e^{j\zeta w}(-1)^m - e^{-j\zeta w}]e^{j\zeta lp}}{\zeta^2 - w_m^2}.$$

Tangential magnetic field continuity on the aperture of the slots at $\rho = b$ is

$$H_\phi^i(b, z) + H_\phi^{s(\mathrm{I})}(b, z) = H_\phi^{(\mathrm{IV})}(b, z). \tag{40}$$

Multiplying both sides of (40) by $\cos w_n(z + w - rp)$ and integrating over the rth slot aperture region, we get

$$\frac{V}{\omega\mu_0 \ln(b/a) b} Q_r^n(-k_1) + \sum_{l=0}^{N-1}\sum_{m=0}^{\infty} \frac{\epsilon_{r1} k_{\rho 4m}}{2\pi\epsilon_{r4}} \cdot \left[b_m^l \frac{H_0^{(1)}(k_{\rho 4m}b)}{H_1^{(1)}(k_{\rho 4m}c)} + c_m^l \frac{H_0^{(2)}(k_{\rho 4m}b)}{H_1^{(2)}(k_{\rho 4m}b)}\right] I_{1,rl}^{nm} = \left[b_n^r \frac{H_1^{(1)}(k_{\rho 4n}b)}{H_1^{(1)}(k_{\rho 4n}c)} + c_n^r\right] \alpha_n w \tag{41}$$

where

$$I_{1,rl}^{nm} = \int_{-\infty}^{\infty} \frac{M_h(\zeta)}{k_{\rho 1} M_e(\zeta)} Q_l^m(\zeta) Q_r^n(-\zeta)\, d\zeta$$

$$M_h(\zeta) = H_1^{(2)}(k_{\rho 1}b) - \frac{H_0^{(2)}(k_{\rho 1}a)}{H_0^{(1)}(k_{\rho 1}a)} H_1^{(1)}(k_{\rho 1}b)$$

and $\alpha_n = 2$, for $n = 0$, $\alpha_n = 1$, for $n \neq 0$. Since the integrand of $I_{1,rl}^{nm}$ contains the poles which correspond to the coaxial waveguide TM modes, the integral can be evaluated in a functional form by use of the Cauchy residue theorem and is given by

$$I_{1,rl}^{nm} = 2\pi w \eta_{1m} \delta_{nm} \delta_{rl} + J_{1,rl}^{nm} \tag{42a}$$

where, as shown in (42b) at the bottom of the next page, λ_p is the solution of $k_{\rho 1} M_e(\zeta)|_{\zeta=\lambda_p} = 0$, and $p = 0$ means the fundamental TEM and $p \neq 0$ the higher order TM modes in coaxial waveguide.

The tangential electric field continuity at $\rho = c$ yields

$$\tilde{H'}_\phi^{s(\mathrm{III})}(\zeta) = \frac{\epsilon_{r3}}{k_{\rho 3} N_e(\zeta)} \sum_{l=0}^{N-1}\sum_{m=0}^{\infty} \frac{k_{\rho 4m}}{\epsilon_{r4}} Q_l^m(\zeta) \cdot \left[b_m^l \frac{H_0^{(1)}(k_{\rho 4m}c)}{H_1^{(1)}(k_{\rho 4m}c)} + c_m^l \frac{H_0^{(2)}(k_{\rho 4m}c)}{H_1^{(2)}(k_{\rho 4m}b)}\right] \tag{43}$$

where

$$N_e(\zeta) = H_0^{(2)}(k_{\rho 3}c) + R(\zeta) H_0^{(1)}(k_{\rho 3}c).$$

Tangential magnetic field continuity on the aperture of the slots

at $\rho = c$ and modes orthogonality give

$$\sum_{l=0}^{N-1}\sum_{m=0}^{\infty}\frac{\epsilon_{r3}k_{\rho 4m}}{2\pi\epsilon_{r4}} \cdot\left[b_m^l\frac{H_0^{(1)}(k_{\rho 4m}c)}{H_1^{(1)}(k_{\rho 4m}c)}+c_m^l\frac{H_0^{(2)}(k_{\rho 4m}c)}{H_1^{(2)}(k_{\rho 4m}b)}\right]I_{2,rl}^{nm} =\left[b_n^r+c_n^r\frac{H_1^{(2)}(k_{\rho 4n}c)}{H_1^{(2)}(k_{\rho 4n}b)}\right]\alpha_n w \tag{44}$$

where

$$I_{2,rl}^{nm}=\int_{-\infty}^{\infty}\frac{N_h(\zeta)}{k_{\rho 3}N_e(\zeta)}Q_l^m(\zeta)Q_r^n(-\zeta)\,d\zeta$$

$$N_h(\zeta)=H_1^{(2)}(k_{\rho 3}c)+R(\zeta)H_1^{(1)}(k_{\rho 3}c).$$

Since the integrand of $I_{2,rl}^{nm}$ contains the surface wave poles and branch points, the integral path can be deformed into a path along the branch cut [4]. The reason for this deformation is to obtain a faster convergent integral. The integral path deformation gives

$$I_{2,rl}^{nm}=2\pi w\eta_{2m}\delta_{mn}\delta_{rl}+J_{2,rl}^{nm} \tag{45}$$

where

$$\eta_{2m}=(1-\delta_{m0})\frac{N_h(\zeta)}{k_{\rho 3}N_e(\zeta)}\bigg|_{\zeta=w_m}$$

$$J_{2,rl}^{nm}=-2\pi j\sum_q Q_{q,rl}^{nm}+J_{2,rl}^{nm\prime}$$

$$Q_{q,rl}^{nm}=\begin{cases}0, & l=r,\ m+n=\text{odd}\\ G(\lambda_q)\dfrac{2\lambda_q^2[1-(-1)^m]\cos 2\lambda_q w]}{(\lambda_q^2-w_m^2)(\lambda_q^2-w_n^2)}, & l=r,\ m=n=0\\ G(\lambda_q)\dfrac{2\lambda_q^2[1-(-1)^m e^{-j2\lambda_q w}]}{(\lambda_q^2-w_m^2)(\lambda_q^2-w_n^2)}, & l=r,\ m+n=\text{even},\ m\neq 0\\ G(\lambda_q)\dfrac{\lambda_q^2 h(\lambda_q)}{(\lambda_q^2-w_m^2)(\lambda_q^2-w_n^2)}, & l\neq r\end{cases}$$

$$J_{2,rl}^{nm\prime}=\begin{cases}0, & l=r,\ m+n=\text{odd}\\ R_1, & l=r,\ m=n,=w_m<k_2\\ R_2+R_2', & l=r,\ m+n=\text{even},\ w_m>k_2\\ R_3+R_3', & l\neq r\end{cases}$$

$$G(\lambda_q)=\lim_{\zeta\to\lambda_q}(\zeta-\lambda_q)\frac{N_h(\zeta)}{k_{\rho 3}N_e(\zeta)}$$

$$R_1=\text{PV}\int_0^{\infty}\frac{N_h(\zeta)}{k_{\rho 3}N_e(\zeta)}\frac{2\zeta^2[1-(-1)^m\cos 2\zeta w]}{(\zeta^2-w_m^2)(\zeta^2-w_n^2)}\,d\zeta$$

$$R_2=4j\int_0^{\infty}\text{Im}\left\{\frac{N_h(\zeta)}{k_{\rho 3}N_e(\zeta)}\bigg|_{\zeta=-j\alpha}\right\}\cdot\frac{\alpha^2[1-(-1)^m e^{-2\alpha w}]}{(\alpha^2+w_m^2)(\alpha^2+w_n^2)}\,d\alpha$$

$$R_2'=4\int_0^{k_2}\text{Im}\left\{\frac{N_h(\zeta)}{k_{\rho 3}N_e(\zeta)}\right\}\frac{\zeta^2[1-(-1)^m e^{-j2\zeta w}]}{(\zeta^2-w_m^2)(\zeta^2-w_n^2)}\,d\zeta$$

$$R_3=2j\int_0^{\infty}\text{Im}\left\{\frac{N_h(\zeta)}{k_{\rho 3}N_e(\zeta)}\bigg|_{\zeta=-j\alpha}\right\}\cdot\frac{\alpha^2 h(-j\alpha)}{(\alpha^2+w_m^2)(\alpha^2+w_n^2)}\,d\alpha$$

$$R_3'=2\int_0^{k_2}\text{Im}\left\{\frac{N_h(\zeta)}{k_{\rho 3}N_e(\zeta)}\right\}\frac{\zeta^2 h(\zeta)}{(\zeta^2-w_m^2)(\zeta^2-w_n^2)}\,d\zeta$$

$$h(\zeta)=[1+(-1)^{m+n}]e^{-j\zeta|l-r|p}-(-1)^m e^{-j\zeta|(l-r)p+2w|}-(-1)^n e^{-j\zeta|(l-r)p-2w|}$$

and λ_q is the solution of $N_e(\zeta)|_{\lambda_q}=0$ which is the well-known modal equation for axial surface wave on a dielectric coated conductor. Using (41) and (44), we can derive following simultaneous linear equations:

$$\begin{bmatrix}\boldsymbol{\Psi}_1 & \boldsymbol{\Psi}_2\\ \boldsymbol{\Psi}_3 & \boldsymbol{\Psi}_4\end{bmatrix}\begin{bmatrix}\mathbf{B}\\ \mathbf{C}\end{bmatrix}=\begin{bmatrix}\mathbf{S}\\ 0\end{bmatrix} \tag{46}$$

where

$$\boldsymbol{\Psi}_{1,rl}^{nm}=\left[\frac{\epsilon_{r1}k_{\rho 4m}}{\epsilon_{r4}}\frac{H_0^{(1)}(k_{\rho 4m}b)}{H_1^{(1)}(k_{\rho 4m}c)}\eta_{1m}w-\frac{H_1^{(1)}(k_{\rho 4n}b)}{H_1^{(1)}(k_{\rho 4n}c)}\alpha_n w\right]\cdot\delta_{mn}\delta_{rl}+\frac{\epsilon_{r1}k_{\rho 4m}}{2\pi\epsilon_{r4}}\frac{H_0^{(1)}(k_{\rho 4m}b)}{H_1^{(1)}(k_{\rho 4m}c)}J_{1,rl}^{nm}$$

$$\boldsymbol{\Psi}_{2,rl}^{nm}=\left[\frac{\epsilon_{r1}k_{\rho 4m}}{\epsilon_{r4}}\frac{H_0^{(2)}(k_{\rho 4m}b)}{H_1^{(2)}(k_{\rho 4m}b)}\eta_{1m}w-\alpha_n w\right]\delta_{mn}\delta_{rl}+\frac{\epsilon_{r1}k_{\rho 4m}}{2\pi\epsilon_{r4}}\frac{H_0^{(2)}(k_{\rho 4m}b)}{H_1^{(2)}(k_{\rho 4m}b)}J_{1,rl}^{nm}$$

$$\boldsymbol{\Psi}_{3,rl}^{nm}=\left[\frac{\epsilon_{r3}k_{\rho 4m}}{\epsilon_{r4}}\frac{H_0^{(1)}(k_{\rho 4m}c)}{H_1^{(1)}(k_{\rho 4m}c)}\eta_{2m}w-\alpha_n w\right]\delta_{mn}\delta_{rl}+\frac{\epsilon_{r3}k_{\rho 4m}}{2\pi\epsilon_{r4}}\frac{H_0^{(1)}(k_{\rho 4m}c)}{H_1^{(1)}(k_{\rho 4m}c)}J_{2,rl}^{nm}$$

$$\boldsymbol{\Psi}_{4,rl}^{nm}=\left[\frac{\epsilon_{r3}k_{\rho 4m}}{\epsilon_{r4}}\frac{H_0^{(2)}(k_{\rho 4m}c)}{H_1^{(2)}(k_{\rho 4m}b)}\eta_{2m}w-\frac{H_1^{(2)}(k_{\rho 4n}c)}{H_1^{(2)}(k_{\rho 4n}b)}\alpha_n w\right]\cdot\delta_{mn}\delta_{rl}+\frac{\epsilon_{r3}k_{\rho 4m}}{2\pi\epsilon_{r4}}\frac{H_0^{(2)}(k_{\rho 4m}c)}{H_1^{(2)}(k_{\rho 4m}b)}J_{2,rl}^{nm}$$

$$\mathbf{S}_r^n=-\frac{Vk_1}{k_0\eta_0\ln(b/a)b}Q_r^n(-k_1).$$

$$\eta_{1m}=\alpha_m\frac{M_h(\zeta)}{k_{\rho 1}M_e(\zeta)}\bigg|_{\zeta=w_m},$$

$$J_{1,rl}^{nm}=-2\pi j\sum_{p=0}^{\infty}\frac{\lambda_p}{b}P(\lambda_p)\frac{[(-1)^{m+n}+1]e^{-j\lambda_p|l-r|p}-(-1)^m e^{-j\lambda_p|(l-r)p+2w|}-(-1)^n e^{-j\lambda_p|(l-r)p-2w|}}{(\lambda_p^2-w_m^2)(\lambda_p^2-w_n^2)},$$

$$P(\lambda_p)=\begin{cases}\dfrac{1}{2\ln(b/a)}, & p=0\\ \dfrac{[J_0(k_{\rho 1}a)]^2}{[J_0(k_{\rho 1}a)]^2-[J_0(k_{\rho 1}b)]^2}\bigg|_{\zeta=\lambda_p}, & p\neq 0\end{cases} \tag{42b}$$

Once the unknown radial waveguide mode coefficients b_m^l and c_m^l are determined by solving (46), $\tilde{H}_\phi^{s(\mathrm{I})}(\zeta)$ and $\tilde{H'}_\phi^{s(\mathrm{III})}(\zeta)$ are computed by (39) and (43), respectively. Hence, all field coefficients are known, the fields in each region can be calculated by the use of the field equations (35)–(38). The wave radiated from the slots are divided into two wave types, i.e., one is the space wave which is radiated into the region (II), and the other the surface wave which is trapped in and above the dielectric and guided in the $\pm z$ directions. The far-zone magnetic field radiated into the region (II), by using an asymptotic evaluation, is given as

$$H_{\phi,\,space}^{(\mathrm{II})}(R,\theta) = \sum_l \sum_m \frac{\epsilon_{r3}k_{\rho 4m}}{\pi\epsilon_{r4}}\left[b_m^l\frac{H_0^{(1)}(k_{\rho 4m}c)}{H_1^{(1)}(k_{\rho 4m}c)} + c_m^l\frac{H_0^{(2)}(k_{\rho 4m}c)}{H_1^{(2)}(k_{\rho 4m}b)}\right] \cdot F_{\mathrm{space}}(k_2\cos\theta)\frac{e^{-jk_2R}}{R} \tag{47}$$

where

$$F_{\mathrm{space}}(\zeta) = -\frac{T(\zeta)}{k_{\rho 3}[H_0^{(2)}(k_{\rho 3}c)+R(\zeta)H_0^{(1)}(k_{\rho 3}c)]}Q_l^m(\zeta)$$

from which the radiation pattern is calculated. The surface wave in each region is calculated by applying the Cauchy residue theorem on the inverse Fourier transformation (36) and (37) and is expressed as

$$H_{\phi,\,surf}^{(\mathrm{II})\pm}(\rho,z) = \mp j\sum_q\sum_l\sum_m \frac{\epsilon_{r3}k_{\rho 4m}}{\epsilon_{r4}} \cdot\left[b_m^l\frac{H_0^{(1)}(k_{\rho 4m}c)}{H_1^{(1)}(k_{\rho 4m}c)} + c_m^l\frac{H_0^{(2)}(k_{\rho 4m}c)}{H_1^{(2)}(k_{\rho 4m}b)}\right] \cdot F_{\mathrm{surf}}^{(\mathrm{II})}(\pm\lambda_q)e^{\mp j\lambda_q z}$$

$$H_{\phi,\,surf}^{(\mathrm{III})\pm}(\rho,z) = \mp j\sum_q\sum_l\sum_m \frac{\epsilon_{r3}k_{\rho 4m}}{\epsilon_{r4}} \cdot\left[b_m^l\frac{H_0^{(1)}(k_{\rho 4m}c)}{H_1^{(1)}(k_{\rho 4m}c)} + c_m^l\frac{H_0^{(2)}(k_{\rho 4m}c)}{H_1^{(2)}(k_{\rho 4m}b)}\right] \cdot F_{\mathrm{surf}}^{(\mathrm{III})}(\pm\lambda_q)e^{\mp j\lambda_q z} \tag{48}$$

where

$$F_{\mathrm{surf}}^{(\mathrm{II})}(\pm\lambda_q) = \lim_{\zeta\to\pm\lambda_q}(\zeta\mp\lambda_q)\frac{T(\zeta)}{k_{\rho 3}[H_0^{(2)}(k_{\rho 3}c)+R(\zeta)H_0^{(1)}(k_{\rho 3}c)]} \cdot Q_l^m(\zeta)H_1^{(2)}(k_{\rho 2}\rho)$$

$$F_{\mathrm{surf}}^{(\mathrm{III})}(\pm\lambda_q) = \lim_{\zeta\to\pm\lambda_q}(\zeta\mp\lambda_q)\frac{H_1^{(2)}(k_{\rho 3}\rho)+R(\zeta)H_1^{(1)}(k_{\rho 3}\rho)}{k_{\rho 3}[H_0^{(2)}(k_{\rho 3}c)+R(\zeta)H_0^{(1)}(k_{\rho 3}c)]} \cdot Q_l^m(\zeta)$$

and the superscript $\pm$ means positive and negative z-direction traveling waves, respectively. The time-averaged incident power (P_{inc}), reflected power (P_r), coupled power to the guide beyond the slotted region (P_t), and transmitted power from slots (P_{rad}) to regions (II) and (III) are given by (49)–(52), shown at the bottom of the page.

In the derivation of the P_{rad}, the conservation of complex power [5], [6] is used. Part of the power P_{rad} through the slots goes into the surface wave guided by the dielectric over the conductor and the balance into space wave. This part is carried in the surface wave is designated P_{surf}, while the part in the space wave is denoted P_{space}, and these powers can be evaluated by using (47) and (48).

V. Numerical Results and Discussion

To be certain that the complex propagation constant ($\beta - j\alpha$) converges to the correct value, we calculate the tangential electric and magnetic fields at the interfaces (at $\rho = b$, c, and d) for a structure having $a = 0.05\lambda$ (free-space wavelength), $b = 0.25\lambda$, $c = 0.3\lambda$, $d = 0.4\lambda$, $p = 0.55\lambda$, $w = 0.25p$, and $\epsilon_{r1} = 2.5$, $\epsilon_{r2} = 1.0$, $\epsilon_{r3} = \epsilon_{r4} = 1.0$ and plot in Fig. 3, when 20 radial waveguide modes and 50 space harmonics for finite thick slot and ten strip-current modes and 50 space harmonics for zero thick slot are employed. The tangential electric fields are identical on both sides of the interfaces and vanish on the metal surfaces. The tangential magnetic fields are continuous over the slot region and discontinuous over the metal region because of the electric current on the

$$P_{inc} = \frac{\pi k_1 V^2}{k_0\eta_0\ln b/a} \tag{49}$$

$$P_r = \frac{\pi\eta_0}{k_0k_1\epsilon_{r1}\ln b/a}\left|\sum_{l=0}^{N-1}\sum_{m=0}^{\infty}\frac{\epsilon_{r1}k_{\rho 4m}}{2\epsilon_{r4}}\left[b_m^l\frac{H_0^{(1)}(k_{\rho 4m}b)}{H_1^{(1)}(k_{\rho 4m}c)} + c_m^l\frac{H_0^{(2)}(k_{\rho 4m}b)}{H_1^{(2)}(k_{\rho 4m}b)}\right]Q_l^m(-k_1)\right|^2 \tag{50}$$

$$P_t = \frac{\pi\eta_0k_1}{k_0\epsilon_{r1}\ln b/a}\left|\frac{Vk_1}{k_0\eta_0} - \sum_{l=0}^{N-1}\sum_{m=0}^{\infty}\frac{j\epsilon_{r1}k_{\rho 4m}}{2\epsilon_{r4}k_1}\left[b_m^l\frac{H_0^{(1)}(k_{\rho 4m}b)}{H_1^{(1)}(k_{\rho 4m}c)} + c_m^l\frac{H_0^{(2)}(k_{\rho 4m}b)}{H_1^{(2)}(k_{\rho 4m}b)}\right]Q_l^m(k_1)\right|^2 \tag{51}$$

$$P_{\mathrm{rad}} = -\pi c\,\mathrm{Re}\left\{\frac{\eta_0}{jk_0\epsilon_{r4}}\sum_{r=0}^{N-1}\sum_{n=0}^{\infty}k_{\rho 4n}\left[b_n^r\frac{H_0^{(1)}(k_{\rho 4n}c)}{H_1^{(1)}(k_{\rho 4n}c)} + c_n^r\frac{H_0^{(2)}(k_{\rho 4n}c)}{H_1^{(2)}(k_{\rho 4n}b)}\right] \times\frac{\epsilon_{r3}}{2\pi\epsilon_{r4}}\left\{\sum_{l=0}^{N-1}\sum_{m=0}^{\infty}k_{\rho 4m}\left[b_m^l\frac{H_0^{(1)}(k_{\rho 4m}c)}{H_1^{(1)}(k_{\rho 4m}c)} + c_m^l\frac{H_0^{(2)}(k_{\rho 4m}c)}{H_1^{(2)}(k_{\rho 4m}b)}\right]\right\}^* I_{2,rl}^{nm*}\right\} \tag{52}$$

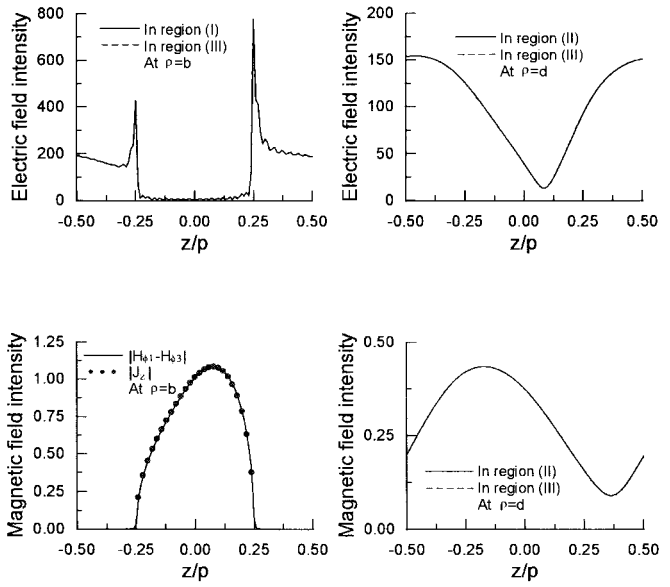

(a)

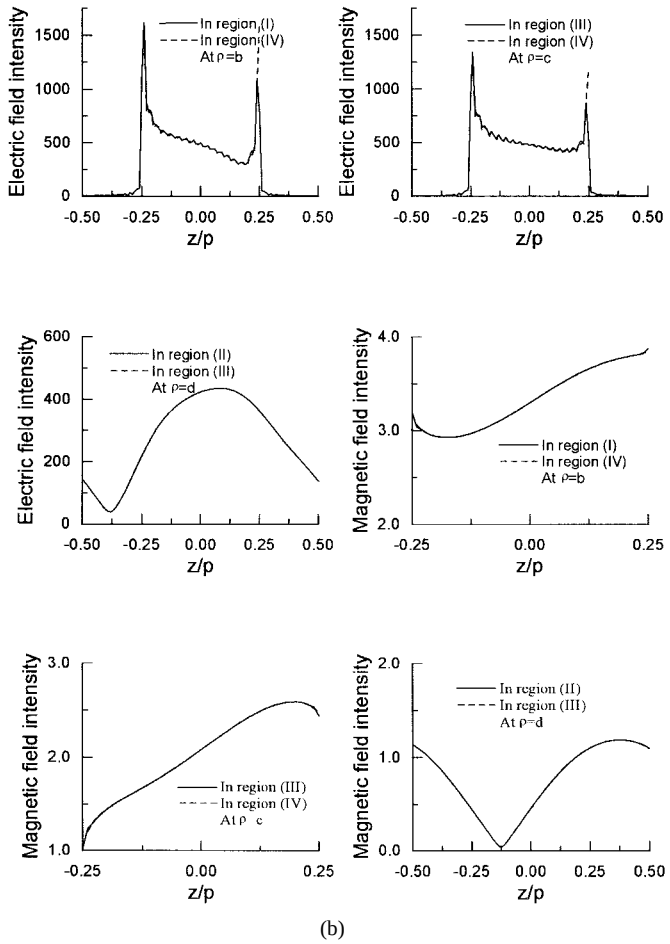

(b)

Fig. 3. Field amplitudes at the interfaces. (a) Zero thickness slot case. (b) Finite thickness slot case: $p = 0.55\lambda$, $a = 0.05\lambda$, $b = 0.25\lambda$, $c = 0.3\lambda$, $d = 0.4\lambda$, $w = 0.25p$, $\epsilon_{r1} = 2.5$, $\epsilon_{r2} = 1.0$, $\epsilon_{r3} = \epsilon_{r4} = 2.0$.

metal surfaces. Fig. 3 shows that the boundary conditions at the interfaces are satisfied and the problem is solved in the corrected manner.

Fig. 4 shows β/k_2 and α/k_2 as a function of the normalized slot thickness $t\ (=c-b)/\lambda$ for dielectric coated and uncoated

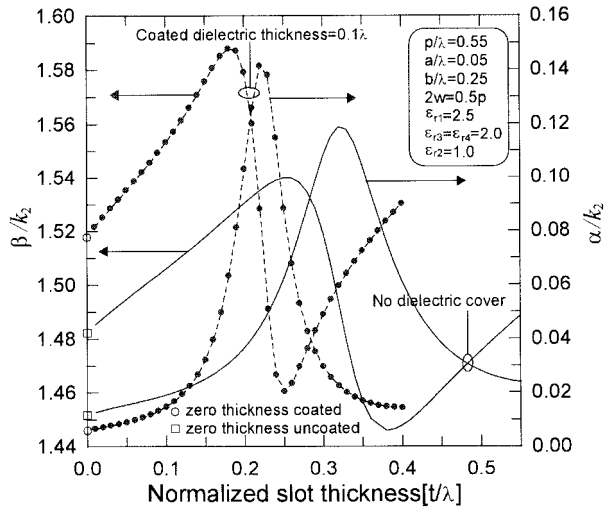

Fig. 4. Variation of β and α with the normalized slot thickness: $p = 0.55\lambda$, $a = 0.05\lambda, 2w = 0.5p, b = 0.25\lambda, \epsilon_{r1} = 2.5, \epsilon_{r2} = 1.0, \epsilon_{r3} = \epsilon_{r4} = 2.0$.

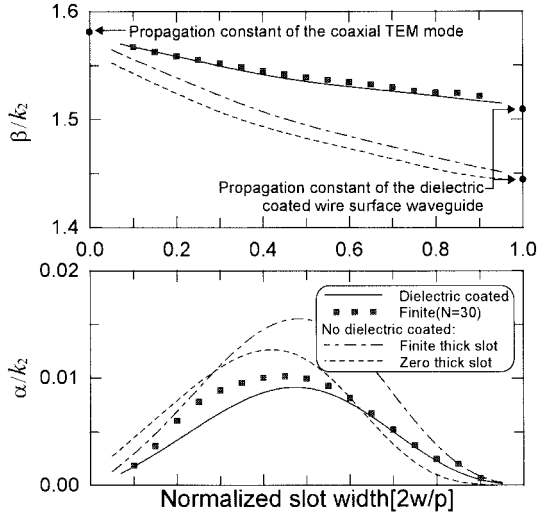

Fig. 5. Comparison of β and α between infinite and finite periodic structure with the normalized slot width as parameter: $p = 0.55\lambda$, $a = 0.05\lambda$, $b = 0.25\lambda$, $c = 0.3\lambda$, $d = 0.4\lambda$, $\epsilon_{r1} = 2.5$, $\epsilon_{r2} = 1.0$, $\epsilon_{r3} = \epsilon_{r4} = 2.0$.

cases. It is shown that the leakage and phase constants oscillate with periodicity as the normalized slot thickness is increased. This is because the slot region can be considered a radial waveguide in which TEM mode can propagate along the ρ direction. The leakage constant increases with slot thickness, but it reaches its maximum value when slot thickness is approximately $0.32\lambda_4$ [wavelength in region (IV)] and decreases again when thickness is increased further. As shown in this figure, the values of the β and α for the zero thickness agree with the ones obtained by mode matching for thin-slot thickness.

The effect of the normalized slot width on the radiation characteristics is shown in Fig. 5. From this figure, it is found that the phase constant monotonically decreases as the slot width increases but the leakage constant goes to a maximum and decreases again as the slot width increases. Since a narrow slot width case corresponds to the periodic slot perturbation of the coaxial waveguide, we can expect that the leakage constant

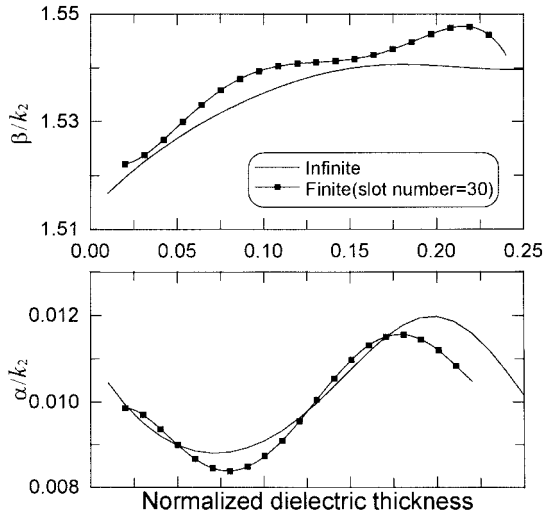

Fig. 6. Comparison of β and α between infinite and finite periodic structure with the normalized dielectric thickness as parameter: $p = 0.55\lambda$, $a = 0.05\lambda$, $b = 0.25\lambda$, $c = 0.3\lambda$, $w = 0.25p$, $\epsilon_{r1} = 2.5$, $\epsilon_{r2} = 1.0$, $\epsilon_{r3} = \epsilon_{r4} = 2.0$.

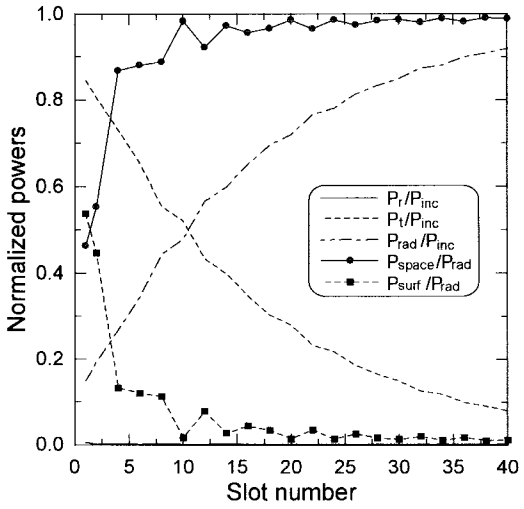

Fig. 8. Normalized powers P_r, P_t, $P_{\rm rad}$, $P_{\rm space}$, and $P_{\rm surf}$ versus total slot number: $p = 0.55\lambda$, $a = 0.05\lambda$, $b = 0.25\lambda$, $c = 0.3\lambda$, $d = 0.4\lambda$, $w = 0.25p$, $\epsilon_{r1} = 2.5$, $\epsilon_{r2} = 1.0$, $\epsilon_{r3} = \epsilon_{r4} = 2.0$.

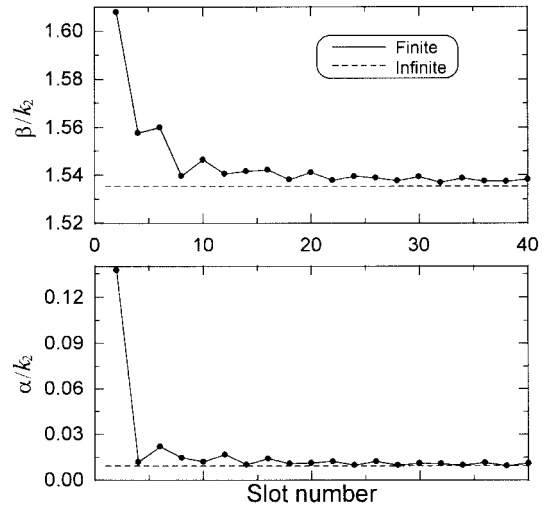

Fig. 7. Variation of β and α with the slot number: $p = 0.55\lambda$, $a = 0.05\lambda$, $b = 0.25\lambda$, $c = 0.3\lambda$, $d = 0.4\lambda$, $w = 0.25p$, $\epsilon_{r1} = 2.5$, $\epsilon_{r2} = 1.0$, $\epsilon_{r3} = \epsilon_{r4} = 2.0$.

will increase as slot width increases. However, a wide slot case can be considered as a periodic metal perturbation of the dielectric-coated wire-surface waveguide. Therefore, the leakage constant decreases as slot width increases and finally disappears. This figure shows that the values of the β and α for the finite 30 periodic slots obtained in an average sense [6], [7] are very well matched to those of the infinite periodic structure.

Fig. 6 shows the effect of the coated dielectric thickness on β/k_2 and α/k_2. It can be seen from the figure that the leakage constant α changes like a sinusoidal function, while the phase constant β has almost no change with the increase of the dielectric thickness. This figure shows good agreement between β and α of the finite periodic slots and those of the infinite periodic structure.

The variation of the complex propagation constant of the finite periodic slots obtained in an average sense is plotted in Fig. 7 for increasing the number of the slot. The complex propagation constant $(\beta - j\alpha)$ of the finite periodic slots is almost the same as the one of the infinite structure when the slot number is larger than 20. Thus, it is expected that the radiation characteristics of the finite periodic slots are very well matched to those of the infinite structure, because the leaky-wave main beam radiation angle is determined by β and 3-dB beamwidth of the leaky-wave antenna related with α.

The validity of the numerical results in this study is assured by a check of the power conservation law

$$P_r + P_t + P_{\rm rad} = P_{\rm inc}$$
$$P_{\rm space} + P_{\rm surf} = P_{\rm rad}.$$

The variation of the powers versus the slot number is shown in Fig. 8. This figure shows that the power conservation law is satisfied for all slot numbers. The surface wave power is larger than the space-wave power for a single slot, but it is reversed as the slot numbers increase. For the case of $N_{slot} = 40$, 91.9% the incident power is radiated into regions (II) and (III), 0.15% is reflected, and 7.95% is transmitted to the guide beyond the slotted region. 98.9 and 1.1% of the radiated power from the slots into regions (II) and (III) are launched into space and surface wave powers, respectively. Thus, when the leaky-wave mode is established in the finite structure, most of the coupled power in the regions (II) and (III) is radiated into region (II) as a space wave (leaky wave) and the surface wave is negligible. This means that the undesired power loss by the surface wave due to the dielectric coating can be ignored in the leaky-wave antenna structure. Therefore, the dielectric coating has almost no effect on the antenna efficiency $(P_{\rm space}/P_{\rm rad})$ due to surface wave, but on the main beam radiation angle and beamwidth of the leaky-wave antenna.

Fig. 9 shows the radiation pattern of the finite periodic slots calculated by (47) compared to the results evaluated by using (26) from the study of an infinite structure. The main beam radiation angle ($\theta_{\max} \approx 106.4°$) and beamwidth ($\approx 2.6°$) are almost the same, but some discrepancies between finite and

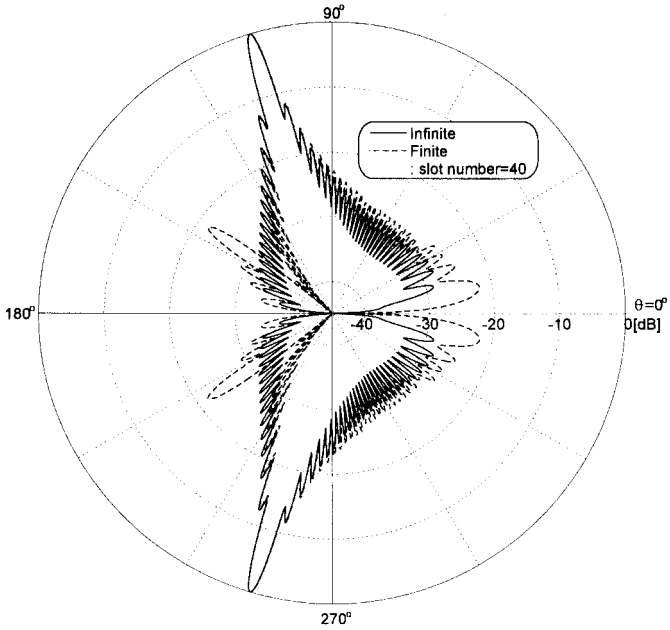

Fig. 9. Radiation pattern: $p = 0.55\lambda$, $a = 0.05\lambda$, $b = 0.25\lambda$, $c = 0.3\lambda$, $d = 0.4\lambda$, $w = 0.25p$, $\epsilon_{r1} = 2.5$, $\epsilon_{r2} = 1.0$, $\epsilon_{r3} = \epsilon_{r4} = 2.0$.

infinite cases are observed in the side lobes. This is due to the effect of the end sections of the finite structure.

VI. Conclusion

The analysis method for the dielectric-coated coaxial waveguide infinite periodic slot with finite and zero thickness as a leaky-wave antenna and the solution method for the leaky wave radiated from the finite periodic slots excited by TEM incident wave are proposed. In this paper, rigorous mode-matching technique and an integral equation formulation are applied to obtain the complex propagation constant of the leaky wave for the finite and zero thickness slots of the infinite periodic structure, respectively. The validity of the proposed method is checked by calculating tangential electromagnetic fields at the interfaces and by all eying the power conservation law. Phase and leakage constants and radiation pattern of the antenna are calculated with slot thickness, slot width and dielectric thickness as parameters. The variations of the complex propagation constant and powers (reflected, transmitted, space, and surface wave powers) of the finite periodic slots are calculated for increasing slot numbers and good agreement is obtained for more than 20 slots. It has been observed that the dielectric coating on the slots has almost no effect on antenna efficiency due to the surface wave, but on the leaky-wave radiation angle and main beamwidth of the antenna. The main beam radiation angle and beamwidth of the finite periodic slots are perfectly matched to those of the infinite structure except for the sidelobes due to the finite end effect. A good agreement between the results of the finite periodic slots and those of the infinite structure has been found. The methods proposed in this paper are thought to be useful in predicting the performance of the leaky-wave antenna at the design stage.

References

[1] S. Xu, J. Min, S. T. Peng, and F. K. Shwering, "A millimeter-wave omnidirectional circular dielectric rod grating antenna," *IEEE Trans. Antennas Propagat.*, vol. 39, pp. 883–891, July 1991.
[2] S. Xu and X. Wu, "A millimeter-wave omnidirectional dielectric rod metal grating antenna," *IEEE Trans. Antennas Propagat.*, vol. 44, pp. 74–79, Jan. 1996.
[3] K. Uchida, T. Noda, and T. Matsunaga, "Electromagnetic wave scattering by an infinite plane metallic grating in case of oblique incidence and arbitrary polarization," *IEEE Trans. Antennas Propagat.*, vol. 36, pp. 415–422, Mar. 1988.
[4] J. R. Wait and D. A. Hill, "On the electromagnetic field of a dielectric coated coaxial cable with an interrupted shield," *IEEE Trans. Antennas Propagat.*, vol. AP-23, pp. 470–479, July 1975.
[5] R. F. Harrington, *Time-Harmonic Electromagnetic Fields.* New York: McGraw-Hill, 1961.
[6] C. W. Lee and H. Son, "Periodically slotted dielectrically filled parallel-plate waveguide as a leaky wave antenna: E-polarization case," *IEEE Trans. Antennas Propagat.*, to be published.
[7] C. W. Lee, J. I. Lee, and Y. K. Cho, "Analysis of leaky waves from a periodically slotted parallel-plate waveguide for a finite number of slots," *Electron. Lett.*, vol. 30, no. 20, pp. 1633–1634, 1994.

Chang-Won Lee was born in Kumi, Korea, on December 13, 1967. He received the B.S., M.S., and Ph.D. degrees in electrical engineering from Kyungpook National University, Taegu, Korea, in 1991, 1993, and 1998, respectively.

His current research interests include analytical and numerical solutions to electromagnetic radiation and scattering problems, printed antennas, periodic structures, and bioelectromagnetics.

Dr. Lee received a URSI Commission B Young Scientist Award at the 1995 Electromagnetic Theory Symposium, St. Petersburg, Russia.

Hyun Son received the B.S.E.E. degree from Yonsei University, Seoul, Korea, the M.S.E.E. degree from Han-Yang University, Seoul, Korea, and the Ph.D. degree in electrical engineering from Kyunghee University, Seoul, Korea, in 1960, 1975, and 1984, respectively.

From 1966 to 1977, he worked for U.S. Armed Forces in the Korean Division of Information and Communication as the Head of Technique. Since 1977 he has been a Professor in the School of Electronics and Electrical Engineering, Kyungpook National University, Taegu, Korea. From 1980 to 1990 he was a Director of Taegu-Kyungpook branch of the Korean Institute of Telemetrics and Electronics. In 1987 he visited the Electronics and Telecommunications Research Institute, Tohoku University, Japan, as a Guest Professor. Since 1991 he has been on the Advisory Committee of the Korean Radio Promotion Association. His current research interests include electromagnetic radiation and scattering problems, mobile communication environment, and satellite communication.

Dr. Son was a Councilor of the Korea Sensors Society from 1992 to 1994. From 1993 to 1994 he was on the Communication Committee of the Ministry of Communications Radio Technology Development. Since 1994 he has been Chairman of IEEE Korea Taegu section.